ELSEVIER

Journal of Power Sources 103 (2001) 61–66

JOURNAL OF POWER SOURCES

www.elsevier.com/locate/jpowsour

A rapid evaluation of vanadium oxide and manganese oxide as battery materials with a micro-electrochemistry technique

V. Vivier*, S. Belair, C. Cachet-Vivier, J.-Y. Nedelec, L.T. Yu

Laboratoire d'Electrochimie, Catalyse et Synthèse Organique, UMR 7582 CNRS, Université Paris Val de Marne, 2 Rue H. Dunant, 94320 Thiais, France

Received 14 April 2001; accepted 25 May 2001

Abstract

The electrochemical behavior of vanadium oxide V_2O_5 and bismuth doped manganese oxide Bi–MnO_2 as battery materials was studied with a cavity microelectrode (CME). This technique, which allows working on a very few amount of material, appears to be suitable when high scan rates are used. Thus, it is possible to perform many hundreds cycles in a short time. The performances of pure vanadium oxide as lithium insertion material in inorganic media, examined with a CME appear to be excellent whereas poor results were obtained with Bi doped MnO_2, for which the electrochemical mechanism proceeds via dissolution.

Keywords: Cavity microelectrode; Battery materials; Vanadium oxide; Manganese oxide

1. Introduction

Battery materials have received a significant attention during the last decades, specially due to the various possible applications such as electrical vehicles, phones, or any other portable devices. These studies were generally carried out with a complete battery [1,2] or with a half electrochemical cell [3,4], with dimensions of at least few square centimeters. The amount of material was between a few milligrams and a few grams. Actually, the most important factor is the electroactive area of the material, which is always much larger than the geometric one. This leads to work with systems characterized by a large electrochemical interface inducing drawbacks such as a high ohmic drop or a non negligible capacitive current. Consequently, the range of the scan rates that can be used in cyclic voltammetry must be drastically reduced. Thus laboratory studies usually consist in recording about tens of cycles (typically less than 200), whereas it appears that a good candidate for battery materials should be rechargeable for more than several thousands of cycles. Some papers report tests performed on cells for more than 1000 cycles [5], and sometimes up to 10,000 cycles [6,7]. However, the duration of experiments largely exceeded several weeks even few months.

In a recent paper, Fiedler [8] reported a study of γ-MnO_2 in an alkaline media by abrasive stripping voltammetry. One of the prominent finding was that the results obtained with such an electrode (a 0.5 mm Pt diameter current collector in which the material is incrusted) exhibited the same trend as those of a conventional AA-sized cells. However, Fiedler mentioned that the scan rate was limited at 2 mV s^{-1} to avoid ohmic drop that distorted voltammograms. Thus, decreasing electrode dimensions appears to be a valuable alternative to probe the rechargeability of battery materials. We have recently developed a cavity microelectrode (CME) able to work with only about 10^{-8} g of electroactive material [9,10]. This electrode was shown to study powder materials with scan rates much higher than 10 mV s^{-1}, allowing electrochemical mechanisms occurring during solid state reactions to be determined [11,12]. Feasibility to study battery materials with CME was demonstrated in a previous paper taking polyaniline as an example [13].

In this paper, we report the possibility to perform hundreds of cycles in a short time with compounds usually considered as battery materials.

We focus our interest on vanadium oxide and manganese oxide for which electrochemical processes are well elucidated. V_2O_5 exhibits a promising behavior as cathodic material for secondary lithium batteries, specially due to its high specific capacity (≈300 mAh g^{-1} [14]). For aqueous system, MnO_2, and more specifically doped manganese oxide (for instance, Bi-doped MnO_2) was investigated. It

* Corresponding author. Tel.: +33-1-49-78-11-37; fax: +33-1-49-78-13-23.
E-mail address: vivier@glvt-cnrs.fr (V. Vivier).

0378-7753/01/$ – see front matter
PII: S0378-7753(01)00822-9

was shown that bismuth incorporation in the manganese oxide structure improved the rechargeability of the matrix by forming a complex [15,16].

2. Experimental

2.1. Preparative procedures

The vanadium pentoxide V_2O_5 was synthesized by a sol–gel process [17,18]. A 0.1 mol l^{-1} metavanadate aqueous solution was passed through a proton exchanged resin to form decavanadic acid. After 24 h at room temperature in a closed bottle, a V_2O_5 gel with formula V_2O_5, nH_2O ($n \approx 200$) was formed [19]. This gel lost most of its water molecules at room temperature forming the vanadium xerogel with formula V_2O_5, $1.6H_2O$. An appropriate heat treatment at 550°C for 5 h led to the formation of crystallized orthorhombic V_2O_5 as determined by X-ray diffraction.

The bismuth manganese oxide was produced by a slow decomposition (during 1 week) of potassium permanganate (0.4 mol l^{-1}) solution containing nitric acid (0.5 mol l^{-1}) and nitrate bismuth $Bi(NO_3)_3$ (0.04 mol l^{-1}) at room temperature [15]. After 1 week, the obtained product was filtered, washed with distilled water and dried under vacuum at 70°C for 24 h. The overall formula deduced from the elemental analysis was $Bi_{0.16}Mn_{2.24}$, $1.68H_2O$. For convenience, this oxide is labeled Bi–MnO_2 in all this paper.

2.2. Electrochemical measurements

The electrochemical experiments were performed in a standard three-electrode cell. The working electrode was a home-made CME [10–12]. It consists of a 25 or 50 μm diameter platinum wire embedded with glass. A microcavity was achieved at the end of the platinum wire by dissolving it in a hot aqua regia solution. The powder material was then introduced in the cavity by using CME as a pestle. A microscope (Olympus BX30) coupled with a digital camera unit (DP10) and a personal computer for image processing was used for controlling the included material before and after the electrochemical experiments. As manganese oxide compounds are not always good electronic conductors, a mixing of graphite and Bi–MnO_2 (20/80) was considered. After electrochemical experiments, the microcavity was unloaded with the help of an ultrasonic treatment in diluted HCl for V_2O_5, and in hydrogen peroxide for Bi–MnO_2.

The electrolytes used to examine lithium insertion in vanadium oxide was 1 mol l^{-1} $LiClO_4$ in propylene carbonate (PC). PC, twice distilled, was purchased from Fluka and used as received. Anhydrous lithium perchlorate was dried under vacuum at 180°C for 12 h. The electrochemical behavior of bismuth doped manganese oxide was studied in a 1 mol l^{-1} KOH aqueous electrolyte.

The reference and counter electrodes were saturated calomel electrode and a 1 cm^2 area Pt disk for experiments performed in aqueous solution, and lithium wire in a separate compartment for both reference and counter electrodes for experiments in PC, respectively. Electrochemical measurements were carried out with an Autolab PGSTAT 30 potentiostat (Eco Chemie).

The electrode was immersed for 30 min in the solution before starting the experiment in order that the whole cavity volume to be filled by the electrolyte.

3. Results and discussion

3.1. V_2O_5

Fig. 1 shows the cyclic voltammogram recorded in the 3–3.8 V/Li/Li^+ range at 500 μV s^{-1} for V_2O_5 powder included in a 25 μm diameter CME. The electrochemical response obtained with a CME appears to be formally similar to the one obtained with a graphite paste electrode or with a thin film at similar scan rates [20]. The cyclic voltammogram displays two well defined reduction peaks C_1 and C_2 located at 3.35 and 3.17 V/Li/Li^+, respectively. They correspond to the solid state reduction of vanadium (+V) into vanadium (+IV) coupled with lithium ion insertion. The reverse sweep is characterized by two anodic peaks A_1 and A_2 at 3.41 and 3.20 V/Li/Li^+, which are found to correspond to the C_1 and C_2 insertion steps, respectively. The electrochemical lithium insertion in sol–gel crystalline V_2O_5 can be described through the two relations (1) and (2) depending on the total insertion ratio.

$$V_2O_5 + xLi^+ + xe \rightleftarrows Li_xV_2O_5 \quad \text{with} \quad 0 < x < 0.4 \qquad (1)$$

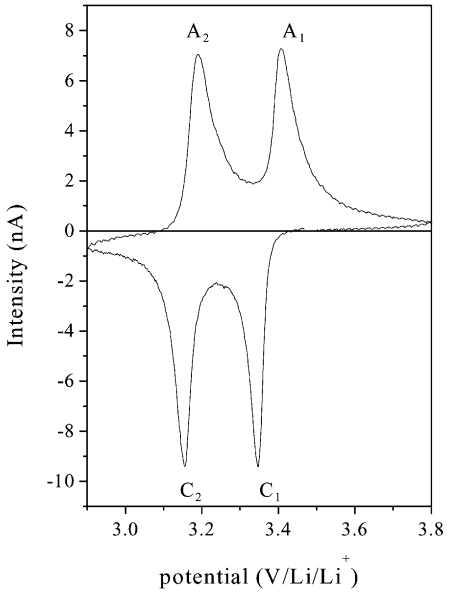

Fig. 1. Cyclic voltammogram recorded on V_2O_5 powder in PC + 1 mol l^{-1} $LiClO_4$ at 500 μV s^{-1} with a 25 μm diameter CME.

$$Li_{0.4}V_2O_5 + yLi^+ + ye \rightleftarrows Li_{0.4+y}V_2O_5 \quad \text{with} \quad 0 < y < 0.6 \tag{2}$$

By analogy with solid solutions of metals, this insertion reaction may be regarded as dissolution reaction, kinetically limited by lithium diffusion in the host material. It is worthwhile to mention that the latter process is responsible for limiting the usable scan rates. Such limitations, intrinsically due to materials properties, can be simply counterbalanced with CME, by reducing electrode dimensions.

The exchanged charge during the two reduction (oxidation) steps is deduced from the area measurement of peaks C_1 and C_2 (A_1 and A_2) with the help of Eq. (3).

$$Q_X = \frac{A_X}{v} \tag{3}$$

where X is the peak label (A_1 or A_2 for anodic peaks and C_1 or C_2 for cathodic peaks) and v the scan rate. Thus, the total anodic and cathodic charges (Q_{ox} and Q_{red}, respectively) are the sum of each partial charge of the related sweep.

$$Q_{ox} = Q_{A1} + Q_{A2} \tag{4}$$

$$Q_{red} = Q_{C1} + Q_{C2} \tag{5}$$

From voltammogram of Fig. 1, the evaluation of the partial exchanged charges indicates that the first and the second reduction steps correspond to 40 and 60% of the total cathodic charge Q_{red}, respectively. In the same way, Q_{A1} and Q_{A2} also represent 40 and 60% of the total anodic charge Q_{ox}. This charge repartition is in good agreement with literature data [14]. As a result, we deduce that the electrochemical behavior of pure vanadium oxide powder studied with a CME is very similar to that of V_2O_5 thin film or V_2O_5 powder in a graphite paste electrode. Moreover, one verifies that the area does not depend on the scan rate in the range 500 μV s^{-1} to 10 mV s^{-1}. We deduce that all the electroactive sites of the material participate to the electrochemical reaction. Therefore, we can carry out significant potentiodynamic cycling at 10 mV s^{-1}.

Fig. 2 shows the first, the 1500th, and some intermediate cycles performed at 10 mV s^{-1} on V_2O_5 inserted in a CME, the diameter and the depth of which are 50 and 20 μm, respectively. Using such a scan rate, one can observe a broadening of each peak, but at first glance, the system exhibits a very good reversibility. This is better illustrated by the Fig. 3, in which the evolution of the anodic and cathodic exchanged charges is reported. During cycling, they vary from 4.4 to 4.2 μC, which corresponds to a slow decrease of less than 5% from the initial value of the specific capacity. To the best of our knowledge, it is the first time that such a scan rate can be used for studying lithium insertion in powder inorganic material in an organic solvent. The 1500 cycles were performed at 10 mV s^{-1} on a potential domain spreading from 2.9 to 3.9 V/Li/Li^+. The total duration of the experiment was then less than 4 days. Assuming

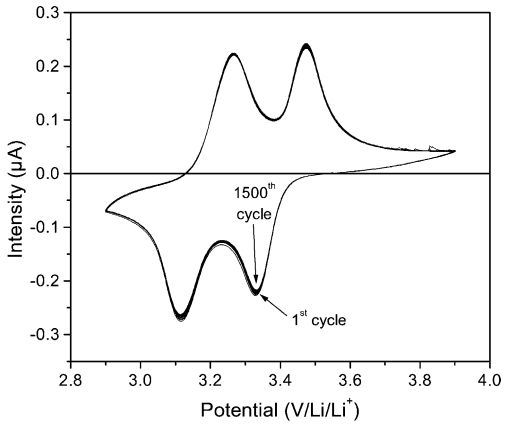

Fig. 2. Cycles (1500) recorded on V_2O_5 powder in PC + 1 mol l^{-1} $LiClO_4$ at 10 mV s^{-1} with a 50 μm diameter CME.

the same test to be performed with a carbon paste electrode, the scan rate to be used should typically be lower than 0.5 mV s^{-1}. Thus, the duration of such an experiment should be at least 2.5 months.

One should also mentioned that when the potential range is extended to lower potential (i.e. when the insertion reaction is examined for insertion rate $x > 1$) the distortion of the compound induced by lithium insertion (phase transformations [14,21]) leads to a rapid fall of the specific capacity from the values corresponding to the first cycles. This is a very similar problem to that observed when working on thin sol–gel crystallized films [20,22]. Nevertheless, the repeated volume variations generated by lithium insertion in the crystalline host material [20] do not modify the total exchanged charge significantly. Thus we conclude that these variations do not promote material expulsion from the cavity to the solution bulk.

Moreover, the peak width remains constant as well as for the anodic peaks (Fig. 4a) than for the cathodic ones

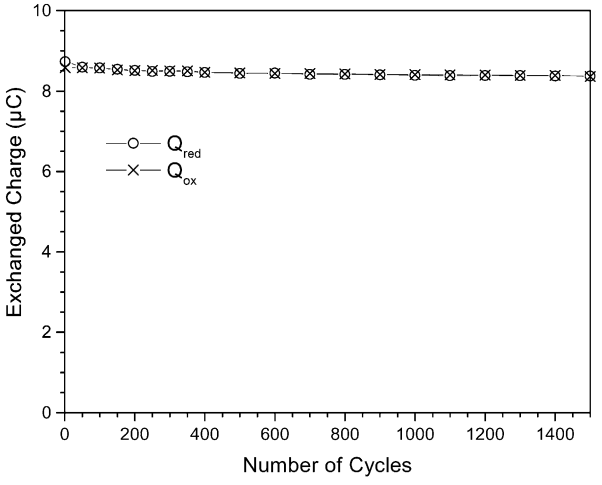

Fig. 3. Evolution of the total anodic and cathodic charges when performing 1500 cycles at 10 mV s^{-1} on V_2O_5 powder in PC + 1 mol l^{-1} $LiClO_4$.

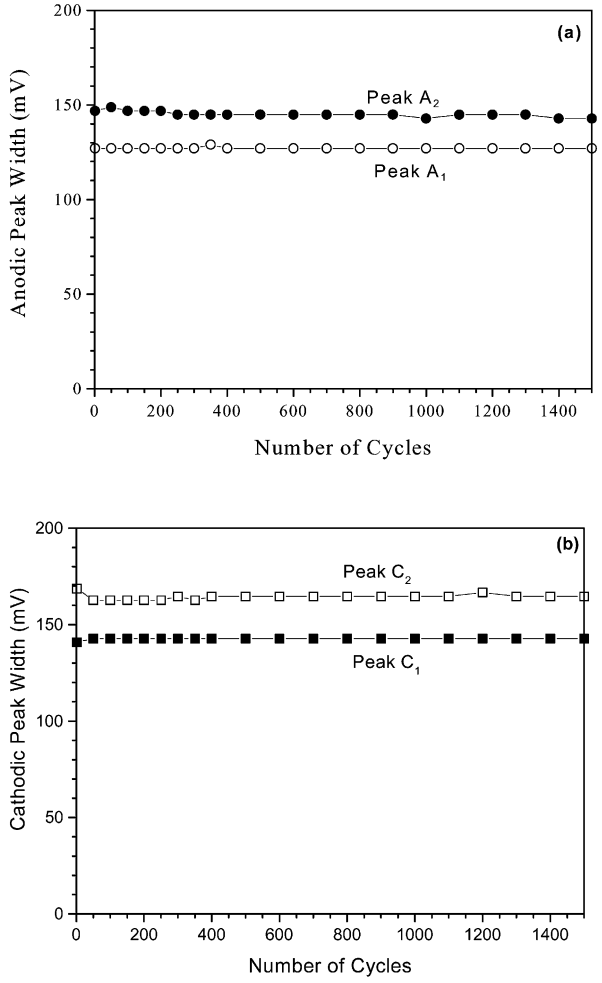

Fig. 4. Evolution of the anodic peak width (a) and the cathodic peak width (b) during 1500 cycles at 10 mV s^{-1} performed on V_2O_5 powder in PC + 1 mol l^{-1} $LiClO_4$.

(Fig. 4b). It means that during cycling, no electrode resistance variation has to be considered, i.e. the contact between two adjacent grains or between grains and platinum collector is sufficient to maintain a good electronic conductivity of the electrode.

Taking into account the unchanging values of both peak intensity and peak width during the whole cycling at a given scan rate, the power that can be supplied by the battery remains constant.

3.2. Bi–MnO_2

In aqueous basic media, the first discharge step of manganese oxide corresponds to the solid state reduction of the compound accompanied by a proton insertion through the overall equilibrium (6).

$$Mn^{(IV)}O_2 + H_2O + e \rightleftarrows Mn^{(III)}OOH + OH^- \quad (6)$$

The dissolution of $Mn^{(III)}OOH$ results in the formation of the intermediate species $Mn^{(III)}(OH)_6^{3-}$. The latter can be reduced in solution as $Mn^{(II)}(OH)_4^{2-}$, to form $Mn^{(II)}(OH)_2$, which precipitates [15,16]. The combination of these intermediate species as shown in Eq. (7) leads to the formation of the spinel Mn_3O_4, which is known to be poorly electroactive and responsible of the poor regenerability of the material.

$$Mn^{(II)}(OH)_2 + 2Mn^{(III)}(OH)_6^{3-} + 6H^+ \rightarrow Mn_3O_4 + 10H_2O \quad (7)$$

When it is added, the bismuth Bi^{3+} prevents the formation of the spinel Mn_3O_4 [15,16,23].

Fig. 5 shows a cyclic voltammogram recorded on a graphite paste electrode (10% Bi–MnO_2/90% graphite) in a 1 mol l^{-1} KOH solution at 0.1 mV s^{-1} within the range −1 to 0.6 V/Hg/HgO. One firstly remarks that the reduction sweep is clearly different from the anodic one. The peak C_3 corresponds to the reduction of Bi^{3+} species (including the Bi–Mn species) in Bi metal. Peaks A_1, A_2 and the diffusion plateau labeled A_3 correspond to a multi-step oxidation of the bismuth formed during the previous reduction sweep [11,24]. The other peaks are related to the reduction or oxidation of the Bi–manganese complexes.

In order to evaluate the performance of Bi–MnO_2 as battery material with a CME, we focus our attention on the range −0.5 to 0.6 V/Hg/HgO, i.e. within a domain where the potential is compatible with a battery electrode use. In Fig. 6 is depicted the five first voltammograms obtained on Bi–MnO_2 at 50 mV s^{-1} with a CME. By comparison with the results obtained with a carbon past electrode, we observe some significant differences mainly attributed to the reduction of electrode dimensions. As a result, the peak resolution as well in reduction as in oxidation are quite better with a CME than with a graphite electrode. For instance, the shoulder C_2 observed after the reduction peak C_1 is to be seen as two different reduction peaks when using microelectrochemistry technique.

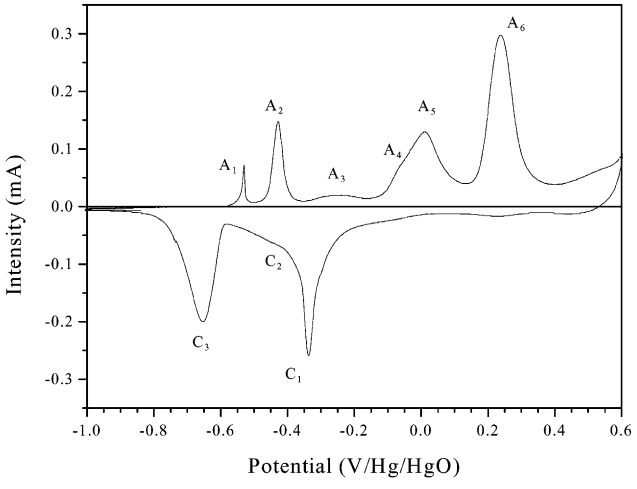

Fig. 5. Cyclic voltammogram of Bi–MnO_2 recorded with a graphite paste electrode (90% graphite and 10% Bi–MnO_2) at 0.1 mV s^{-1} in 1 mol l^{-1} KOH.

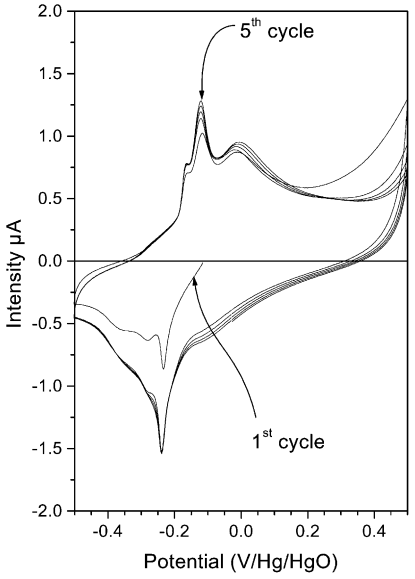

Fig. 6. Five first cycles obtained on Bi–MnO_2 with a CME at 50 mV s^{-1} in 1 mol l^{-1} KOH.

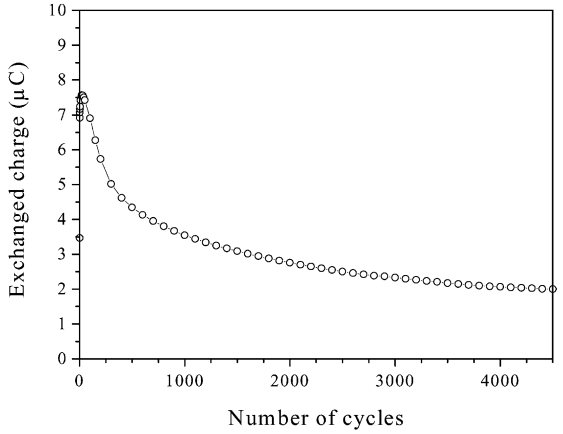

Fig. 7. Evolution of the total exchanged charge during 4500 cycles performed on Bi–MnO_2 with a CME at 50 mV s^{-1}.

We report in Fig. 7 the evolution of the total exchanged charge during 4500 successive sweeps at 50 mV s^{-1} (this scan rate is in the range for which all electroactive sites of the whole material included in the cavity are reacting). The charge increases during the first 20 cycles to reach its maximum value. The exchanged charge represents 50% of the maximum value after 1000 cycles, and only 25% after 4500 cycles. These poor results may be attributed first, to the diffusion of the dissolved species from the cavity to the solution bulk, second, to the formation of Mn_3O_4 not totally hindered in spite of the presence Bi element.

Nevertheless, if a few hundred cycles are aimed at, Bi doped MnO_2 can constitute a valuable candidate for rechargeable batteries in aqueous media, because it is a cheap material when comparison is done with Ni element for instance.

4. Conclusion

The stable electrochemical behavior observed for V_2O_5 during 1500 cycles performed at 10 mV s^{-1} allows to conclude that V_2O_5 is a good candidate as battery material. It must be noticed that this study was made without adjunction of any binder or current collector such as teflon and graphite. Thus, the presence of grain boundaries cannot be responsible for the capacity lost sometimes observed when working on powder and is not to be seen as an obstacle for the study of intercalation materials when it is pure.

The results obtained on bismuth doped manganese oxide are in good accordance with the literature data. This is an interesting finding, because the use of high scan rates (for solid state compounds) when studying the electrochemistry of materials may hid a chemical event (dissolution, complex formation, etc.) if its kinetics is slow regards to the scan rates.

As battery material, the long cycling performance of Bi–MnO_2 is very poor by comparison with this of V_2O_5. The use of a CME appears to be a suitable technique to get a preliminary overview of the battery materials behavior. It allows to distinguish the effects due to the material corrosion from the modifications resulting from charge/discharge processes.

References

[1] J.B. Bates, G.R. Gruzalski, N.J. Dudney, C.F. Luck, X. Yu, Solid-State Ionics 619 (1994) 70–71.
[2] J.B. Bates, G.R. Gruzalski, N.J. Dudney, C.F. Luck, X. Yu, S.D. Jones, Solid State Technol. 36 (1993) 59.
[3] H. Ouboumour, C. Cachet, M. Bode, L.T. Yu, J. Electrochem. Soc. 142 (1995) 1061.
[4] J. Farcy, R. Messina, J. Perichon, J. Electrochem. Soc. 137 (1990) 1337.
[5] J.B. Bates, N.J. Dudney, D.C. Lubben, G.R. Gruzalski, B.S. Kwak, X. Yu, R.A. Zhur, J. Power Sources 54 (1995) 58.
[6] S.D. Jones, J.R. Akridge, J. Power Sources 505 (1993) 43–44.
[7] S.D. Jones, J.R. Akridge, J. Power Sources 54 (1995) 63.
[8] D.A. Fiedler, J. Solid State Electrochem. 2 (1998) 315.
[9] C.S. Cha, C. M Li, H.X. Yang, P.F. Liu, J. Electroanal. Chem. 368 (1994) 47.
[10] V. Vivier, C. Cachet-Vivier, B.L. Wu, C.S. Cha, J.-Y. Nedelec, L.T. Yu, Electrochem. Solid-State Lett. 2 (1999) 385.
[11] V. Vivier, C. Cachet-Vivier, S. Mezaille, B.L. Wu, C.S. Cha, J.-Y. Nedelec, M. Fedoroff, D. Michel, L.T. Yu, J. Electrochem. Soc. 147 (2000) 4252.
[12] V. Vivier, A. Régis, G. Sagon, J.-Y. Nedelec, L.T. Yu, C. Cachet-Vivier, Electrochim. Acta 46 (2001) 907.
[13] V. Vivier, C. Cachet-Vivier, C.S. Cha, J.-Y. Nedelec, L.T. Yu, Electrochem. Commun. 2 (2000) 180.
[14] C. Delmas, H. Cognac-Auradou, J.M. Cocciantelli, M. Ménétrier, J.P. Doumerc, Solid-State Ionics 69 (1994) 257.
[15] M. Bode, C. Cachet, S. Bach, J.-P. Pereira-Ramos, J.L. Ginoux, L.T. Yu, J. Electrochem. Soc. 144 (1997) 792.
[16] L.T. Yu, J. Electrochem. Soc. 144 (1997) 802.
[17] J. Livage, Chem. Mater. 3 (1991) 578.
[18] F. Coustier, J. Hill, B.B. Owens, S. Passerini, W.H. Smyrl, J. Electrochem. Soc. 146 (1999) 1355.

[19] J. Lemerle, N. Nejem, J. Lefebvre, J. Inorg. Nucl. Chem. 42 (1980) 17.
[20] V. Vivier, J. Farcy, J.P. Pereira-Ramos, Electrochim. Acta 44 (1998) 831.
[21] K. West, B. Zachau-Christiansen, T. Jacobsen, S. Skaarup, Solid-State Ionics 76 (1995) 15.
[22] E. A Meulenkamp, W. van Klinken, A.R. Schlatmann, Solid-State Ionics 126 (1999) 235.
[23] Kh.S. Abou-El-Sherbini, M.H. Askar, R. Schollhorn, Solid-State Ionics 139 (2001) 121.
[24] A.M. Espinoza, M.T. San Jose, M.L. Tascon, M.D. Vazquez, P. Sanchez-Batanero, Electrochim. Acta 39 (1991) 1561.